FULL PAPER

Dalton
www.rsc.org/dalton

Syntheses, crystal structures and isomerization kinetics of a series of $[Co(dtc)_2\{P(OMe)_{3-n}Ph_n\}_2]^+$ (n = 0–2) complexes (dtc^- = *N,N*-dimethyldithiocarbamate): role of σ-donicity, π-acidity, and cone angle of the P-ligands in the *trans* influence and *trans* effect †

Satoshi Iwatsuki,[a] Shinsaku Kashiwamura,[a] Kazuo Kashiwabara,[a] Takayoshi Suzuki *[b] and Hideo D. Takagi *[a]

[a] *Department of Chemistry, Graduate School of Science and Research Center for Materials Science, Nagoya University, Nagoya 464-8602, Japan*

[b] *Department of Chemistry, Graduate School of Science, Osaka University, Toyonaka 560-0043, Japan*

Received 12th February 2003, Accepted 10th April 2003
First published as an Advance Article on the web 29th April 2003

A series of geometrical isomers of the new cobalt(III) complexes containing $P(OMe)_{3-n}Ph_n$ (n = 0, 1 or 2), *trans*- and *cis*-$[Co(dtc)_2\{P(OMe)_{3-n}Ph_n\}_2]^+$ (dtc^- = *N,N*-dimethyldithiocarbamate), have been synthesized and the crystal structures and spectrometric properties were obtained. By comparison with reported structures of related $[Co(dtc)_2(P\text{-ligand})_2]^+$ complexes, it was shown that the Co–P bond lengths in $[Co(dtc)_2(P\text{-ligand})_2]^+$ were linearly dependent on the Tolman's cone angle, θ_T, of the P-ligands. On the other hand, the Co–P bond lengths as well as the transition energies of the splitting component ($^1A_{1g} \longrightarrow a^1E_g$: D_{4h}) of the first d–d band of *trans*-$[Co(dtc)_2(P\text{-ligand})_2]^+$ were not linearly dependent on the Tolman's electronic parameter (χ) of the P-ligands. In the *trans*-isomers, it was found that the mutual electronic *trans* influence was not significant in the $[Co(dtc)_2\{P(OMe)_{3-n}Ph_n\}_2]^+$ species while it was far more evident in the complexes with strong σ-donating phosphines such as PMe_3 and PMe_2Ph. A reversible *cis–trans* inter-conversion was observed for the $[Co(dtc)_2\{P(OMe)_{3-n}Ph_n\}_2]^+$ complexes: *cis* to *trans* isomerization was induced by irradiation of light while slow thermal *trans* to *cis* isomerization was observed as a dark reaction. Kinetic measurements of thermal *trans* to *cis* isomerization reactions revealed that the absorption change with time followed multi-exponential kinetics when no free P-ligand was added to the reaction mixture: by addition of excess amounts of free P-ligand, first-order kinetic traces were observed for all reactions. The apparent first-order rate constants were independent of the concentration of added free ligands for the isomerization reactions of $[Co(dtc)_2\{P(OMe)_2Ph\}_2]^+$ and $[Co(dtc)_2\{P(OMe)Ph_2\}_2]^+$, while saturation kinetics were observed for the reaction of $[Co(dtc)_2\{P(OMe)_3\}_2]^+$: all isomerizations involved pre-dissociation of one of the coordinated P-ligands. It was indicated that a significant amount of square pyramidal $[Co(dtc)_2\{P(OMe)_3\}]^+$ exists in equilibrium with $[Co(dtc)_2\{P(OMe)_3\}_2]^+$, while merely a trace amount of such a 5-coordinate species was involved in the reactions of $[Co(dtc)_2\{P(OMe)_2Ph\}_2]^+$ and $[Co(dtc)_2\{P(OMe)Ph_2\}_2]^+$. A contradictory phenomenon observed in these complexes, a small static *trans* influence with a significant kinetic *trans* effect, was explained by the combination of (1) a lack of strong σ-donicity of $P(OMe)_{3-n}Ph_n$ and (2) stabilization of the 5-coordinate square-pyramidal geometry through the electron sponge effect by the dtc^- ligand.

Introduction

Preparations and characterization of mixed-ligand dithiocarbamatocobalt(III) complexes with various P-ligands (ligands with phosphorus atoms at their coordination sites) have been reported to date.[1–9] In particular, their cobalt(III)–bis(phosphite) complexes (phosphite = $P(OMe)_3$, $P(OEt)_3$, and $P(OCH_2)_3CEt$) are examples of rare air-stable compounds with cobalt(III)–phosphite bonds.[5] These phosphite ligands are expected to exhibit weak σ-donicity, while π-acidity of these phosphites are believed to be high.[5] In the previously reported studies of various $[Co(dtc)_2(P\text{-ligand})_2]^+$ complexes (dtc^- = *N,N*-dimethyldithiocarbamate),[1–9] it was observed that the bond lengths between cobalt(III) and P were not related to the Tolman's electronic parameter of each ligand.

We recently succeeded in the determination of crystallographic structures for *cis*- and *trans*-bis(diphenylphosphine) ($PHPh_2$) complexes containing the dtc^- ligand:[9] it was indicated that $PHPh_2$ exhibits relatively strong π-acidity and that the interplay of Tolman's cone angle, σ-donicity and π-acidity, together with the electron sponge effect of dtc^- determines the stability of the complex and the bond length between cobalt(III) and P, although Giering and co-workers had suggested that the π-acidity of $PHPh_2$ is negligibly small.[10] We also reported the thermal *trans* to *cis* isomerization reaction of *trans*-$[Co(dtc)_2(PHPh_2)_2]^+$ in acetonitrile:[9a] although such thermal isomerization reactions of octahedral complexes have been known to take place either through the twist mechanism or through dissociation of one of the coordinated ligands,[11] it was clearly shown that the activation enthalpies for the dissociative isomerization process that involves stereochemical change from the square pyramidal intermediate to the trigonal bipyramidal transition state was much higher than that for the twist process in the case of inert low-spin d^6 metal complexes.[12,13] In addition, we also reported that the *trans*-$[Co(dtc)_2(PHPh_2)_2]^+$ complex very slowly releases coordinated $PHPh_2$.[9a] Such a tendency was also explained by the relatively strong π-interaction between Co(III) and P, as the σ-donicity of $PHPh_2$, represented by the pK_a value of the conjugate acid as well as Tolman's electronic parameter, is very small.[10] However, it should be noted that the

† Electronic supplementary information (ESI) available: bond lengths and angles for all of the *trans*- and *cis*-complexes are summarized in Table S1–S6. The structures of the *trans*-isomers with different orientations and conformations of the OMe and Ph substituents on the P atoms are shown in Figs. S1–S3. See http://www.rsc.org/suppdata/dt/b3/b301712e/

DOI: 10.1039/b301712e

Table 1 Results of the elemental analyses and the ^{1}H NMR signals (δ) for the N–CH_3 (dtc^-) and O–CH_3 (POMe) groups

Complex	Elemental analyses, found (calcd) (%)			^{1}H NMR signals (δ)[a]	
	C	H	N	N–CH_3 (dtc^-)	O–CH_3 (POMe)
cis-$[Co(dtc)_2\{P(OMe)_3\}_2]PF_6$	20.84 (20.81)	4.62 (4.37)	4.07 (4.05)	3.24, 3.28	3.86 (t)
cis-$[Co(dtc)_2\{P(OMe)_2Ph\}_2]PF_6$	33.51 (33.68)	4.28 (4.37)	3.50 (3.57)	2.96, 2.99	3.84 (t), 3.92 (t)
cis-$[Co(dtc)_2\{P(OMe)Ph_2\}_2]PF_6$	42.82 (43.84)	4.36 (4.37)	3.34 (3.20)	2.83, 2.88	3.33 (filled-in d)
trans-$[Co(dtc)_2\{P(OMe)_3\}_2]PF_6$	20.40 (20.81)	3.73 (4.37)	3.86 (4.06)	3.31	3.79 (t)
trans-$[Co(dtc)_2\{P(OMe)_2Ph\}_2]PF_6$	33.60 (33.68)	4.14 (4.37)	3.50 (3.57)	2.99	3.70 (t)
trans-$[Co(dtc)_2\{P(OMe)Ph_2\}_2]PF_6$	43.87 (43.84)	4.20 (4.37)	3.15 (3.20)	2.72	3.62 (t)

[a] In $CDCl_3$ at 30 °C. The term "filled-in doublet" is used to describe a distorted triplet with a broad central peak.

dissociation tendency of $PHPh_2$ in *trans*-$[Co(dtc)_2(PHPh_2)_2]^+$, although it is very slow (10^{-4}–10^{-5} s^{-1} at 333 K), cannot be expected from the relatively short bond length between cobalt(III) and $PHPh_2$,[9a] as it is known that *trans*-$[Co(dtc)_2(PMe_3)_2]^+$ in which the average Co(III)–P bond length (2.287 Å) is longer than that in *trans*-$[Co(dtc)_2(PHPh_2)_2]^+$ (2.276 Å), does not undergo either dissociation of coordinated PMe_3 or isomerization to the *cis* complex.[8]

Historically, the *trans* influence by which a metal to ligand bond *trans* to the particular donor atom that is strongly bound to the metal center suffers elongation has been suggested to be related to the ground-state property inherent in such complexes, while the *trans* effect by which lability of a ligand *trans* to a particular donor atom increases has been related to both ground state and transition-state characteristics.[14] Therefore, *trans* influence and *trans* effect are not necessarily related to each other: to fully understand these two phenomena it is necessary to examine the metal–ligand bond lengths and lability of metal complexes with a series of ligands possessing different donor/acceptor properties.

In this study, we successfully synthesized a series of $[Co(dtc)_2\{P(OMe)_{3-n}Ph_n\}_2]^+$ complexes (n = 0–2), and the crystal structures of both *cis*- and *trans*-isomers for this series of complexes were obtained. The spectrophotometric and NMR data were also collected for the purpose of examining the *static* Co–P interactions, while the *trans* to *cis* isomerization reactions of these complexes were studied for the purpose of examining the *kinetic* stability of the Co–P bonds. The pK_a values of the conjugate acids for $P(OMe)_3$, $P(OMe)_2Ph$, and $P(OMe)Ph_2$ are 2.60, 2.64, and 2.69, while Tolman's electronic parameters, χ, for these ligands are 24.10, 19.45, and 16.30, respectively.[10] Therefore, the σ-donicities of these three ligands are similar to each other, while the χ parameters drastically decrease in the order given. It is also known that the cone angle for $P(OMe)Ph_2$ is the largest, 132°, and it decreases to 115° and 107° for $P(OMe)_2Ph$ and $P(OMe)_3$, respectively.[15] Moreover, the χ parameter for $PHPh_2$ lies between those for $P(OMe)_2Ph$ and $P(OMe)Ph_2$, 17.35, while the pK_a for $PHPh_2$ is much smaller, 0.03, compared with those for these three phosphites.[10] The structure and reactivity for *trans*- and *cis*-$[Co(dtc)_2\{P(OMe)_{3-n}Ph_n\}_2]^+$ was compared with those for previously reported *trans*- and *cis*-$[Co(dtc)_2(P\text{-ligand})_2]^+$ and *trans*- and *cis*-$[Co(acac)_2(P\text{-ligand})_2]^+$ complexes to shed light on the exact nature of the Co–P interactions and the role of the spectator ligand.

Experimental

Syntheses

General procedures. The phosphorus ligands, $P(OMe)_{3-n}Ph_n$, purchased from Aldrich Inc. or Wako Pure Chemicals Inc. were used without further purification and handled under an atmosphere of argon using standard Schlenk techniques until they formed the air-stable cobalt(III) complexes. All of the solvents used in the preparation were deaerated with argon immediately before use.

Preparation of complexes

***cis*-[Co(dtc)$_2${P(OMe)$_{3-n}$Ph$_n$}$_2$](PF$_6$ or BF$_4$) (n = 0, 1 and 2).** The literature method[5] for the preparation of *cis*-$[Co(dtc)_2\{P(OCH_2)_3CEt\}_2]BF_4$ was somewhat modified as follows. To an ice-cold methanol solution (300 cm^3) containing $Co(BF_4)_2\cdot 6H_2O$ (0.85 g, 2.5 mmol) and $P(OMe)Ph_2$ (2.3 g, 10 mmol) added dropwise was an ice-cold solution of tetramethylthiuram disulfide (0.31 g, 1.3 mmol) in a mixture of dichloromethane (10 cm^3) and tetrahydrofuran (50 cm^3) with stirring over 20 min. The mixture was stirred in an ice bath for a further 2 h, and the resulting red brown solution was evaporated to dryness under reduced pressure. The residue was extracted with a small amount of methanol, leaving a green precipitate of $[Co(dtc)_3]$ behind. The filtered red brown extract was placed on a column (7 × 35 cm) of Sephadex LH-20 resin. The adsorbed products were eluted with methanol, affording a major red brown band together with several minor bands. The reddish brown band was collected and concentrated to 20 cm^3 under reduced pressure. Addition of excess NH_4PF_6 to the concentrated reddish brown solution yielded red brown crystals, which were washed with diethyl ether (20 cm^3) and air-dried. Yield: 0.54 g (25%). The corresponding $P(OMe)_2Ph$ and $P(OMe)_3$ complexes were also prepared by a similar method and the yield was 10–20%. Elemental analyses are listed in Table 1, together with the ^{1}H NMR chemical shifts of the signals due to the CH_3 group in dtc^- and P–OCH_3.

***trans*-[Co(dtc)$_2${P(OMe)$_{3-n}$Ph$_n$}$_2$](PF$_6$ or BF$_4$) (n = 0, 1 and 2).** The *trans*-$[Co(dtc)_2\{P(OMe)_{3-n}Ph_n\}_2]PF_6$ complexes were deposited by irradiation of a methanol solution containing the *cis*-isomer and excess NH_4PF_6 with a high-pressure mercury lamp. The yield was 40–50%. The elemental analyses and the ^{1}H NMR data of the complexes are listed in Table 1. It was also possible to prepare the *trans*-$[Co(dtc)_2\{P(OMe)_{3-n}Ph_n\}_2]BF_4$ complexes by the reactions of $P(OMe)_{3-n}Ph_n$ (n = 0, 1 or 2) with *trans*-$[Co(dtc)_2(PPh_3)_2]BF_4$:[8] the yield was *ca.* 50%. An attempt to isolate *trans*-$[Co(dtc)_2\{P(OMe)_2Ph\}_2]BF_4$ and *trans*-$[Co(dtc)_2\{P(OMe)_3\}_2]BF_4$ by an identical column separation method to that employed for the preparation of *cis*-isomers was also successful. The yield of *trans*-$[Co(dtc)_2\{P(OMe)_2Ph\}_2]BF_4$ was 78%, while the yield of *trans*-$[Co(dtc)_2\{P(OMe)_3\}_2]BF_4$ was significantly reduced to 39% under the same conditions.

X-Ray crystallographic study

Single crystals of *cis*-$[Co(dtc)_2\{P(OMe)_3\}_2]BF_4$ were obtained from methanol and those of *cis*-$[Co(dtc)_2\{P(OMe)_2Ph\}_2]PF_6$ and *cis*-$[Co(dtc)_2\{P(OMe)Ph_2\}_2]PF_6$ were deposited by slow evaporation of a dichloromethane/methanol solution at room temperature, while *trans*-$[Co(dtc)_2\{P(OMe)_3\}_2]BF_4$ and *trans*-$[Co(dtc)_2\{P(OMe)_2Ph\}_2]BF_4\cdot(CH_3)_2CO$ deposited as crystals by diffusion of diethyl ether vapor into an acetone solution. Thin plate crystals of *trans*-$[Co(dtc)_2\{P(OMe)Ph_2\}_2]BF_4\cdot 0.5CH_3OH$ were obtained by diffusion of diethyl ether vapor into a methanol solution containing a few drops of acetone in a refrigerator. Each crystal suitable for an X- ray diffraction study was glued on top of a glass fiber with epoxy resin. Except for

trans-[Co(dtc)$_2${P(OMe)Ph$_2$}$_2$]BF$_4$·0.5CH$_3$OH, the X-ray diffraction data were collected at 23(2) °C on a Rigaku AFC-5R four circle diffractometer equipped with graphite-monochromated Mo-K$_\alpha$ radiation (λ = 0.71073 Å). Final lattice parameters were determined by least-squares treatment using setting angles of 25 reflections in the range of 27 < 2θ < 30°. The intensities were corrected for Lorentz-polarization factors and for absorption effects either by the numerical integration method[16] or by the empirical method using three sets of Ψ-scan data.[17] The diffraction data of *trans*-[Co(dtc)$_2${P(OMe)Ph$_2$}$_2$]BF$_4$·0.5CH$_3$OH were obtained at 23(2) °C on a Rigaku Mercury CCD detector with graphite-monochromated Mo-K$_\alpha$ radiation (λ = 0.71073 Å). A total of 1940 images with an oscillation angle of ω = 0.2° were collected with 5 different goniometer settings (8 < 2θ < 55°, exposure time = 15 s). Data were processed by the CrystalClear program package,[18] and the lattice parameters were determined by least-squares treatment using the setting angles of all observed reflections. Absorption corrections were applied by the multi-scan method.[19] The structures were solved by direct methods using the SHELXS86[20] or SHELXS97[21] programs, and refined on F^2 (with all independent reflections) using the SHELXL97 program[21] with anisotropic thermal parameters for all non-hydrogen atoms. H atoms were introduced at the theoretically calculated positions and treated with riding models. All calculations were carried out using the TeXsan software package.[22] Crystallographic data are collected in Table 2, and selected bond lengths and angles obtained for all complexes are summarized in Table 3.

CCDC reference numbers 206913–206918.

See http://www.rsc.org/suppdata/dt/b3/b301712e/ for crystallographic data in CIF or other electronic format.

Measurements

The NMR spectra were obtained in chloroform-*d* at 30 °C on a JEOL Lambda 500 spectrometer. UV-Vis absorption spectra in dichloromethane were measured with a Perkin- Elmer Lambda 19 spectrophotometer at room temperature. For the kinetic measurements in acetonitrile-d_3, a Bruker AMX400WB spectrometer was used at controlled temperatures. Kinetic measurements of the isomerization reactions were also monitored under an Ar atmosphere by JASCO V-560, V-570, Shimadzu UV-1600, and Hitachi U-3400 UV-VIS-NIR spectrophotometers. The temperature of all sample solutions was held constant within ± 0.2 K. Acetonitrile used for the kinetic measurements was obtained from Wako Pure Chemicals Inc., and purified by distillation from phosphorus pentoxide. The amount of residual water in thus purified acetonitrile was examined by a Mitsubishi Kasei CA01 Karl-Fisher apparatus, by which it was determined to be *ca*. 1 mmol kg^{-1}. Trace amounts of water (*ca*. < 10 mmol kg^{-1}) introduced into the sample solutions during preparation are mentioned as "impure water" throughout this article, otherwise the solvent is very pure. Tetra-*n*-butylammonium tetrafluoroborate (0.1 mol kg^{-1}) was used to adjust the ionic strength. All sample solutions were prepared under an inert atmosphere of Ar.

Results and discussion

Preparations

The *cis*-[Co(dtc)$_2${P(OMe)$_2$Ph or P(OMe)Ph$_2$}$_2$]PF$_6$ complexes were prepared by a similar method to that previously reported for *cis*-[Co(dtc)$_2$ (phosphite)$_2$]BF$_4$ (phosphite = P(OMe)$_3$, P(OEt)$_3$ or P(OCH$_2$)$_3$CEt)[5] and for *cis*-[Co(dtc)$_2$(PHPh$_2$)$_2$]BF$_4$.[9] The reaction of a mixture of Co(BF$_4$)$_2$·6H$_2$O and P(OMe)$_{3-n}$Ph$_n$ (n = 0–2) in methanol with tetramethylthiuram disulfide in a molar ratio of 2 : 8 : 1 afforded *cis*-[Co(dtc)$_2${P(OMe)$_{3-n}$Ph$_n$}$_2$]$^+$, which was isolated as the PF$_6^-$ salt with yields of 10–25%. It was not possible to improve the yield because of the preferential formation of [Co(dtc)$_3$]. This preparative method did not produce the corresponding *trans* isomer, which is in contrast to the case of analogous PMe$_2$Ph and PMePh$_2$ complexes.[8]

It was possible to efficiently prepare the *trans*-isomers by the reactions of P(OMe)$_{3-n}$Ph$_n$ with *trans*-[Co(dtc)$_2$(PPh$_3$)$_2$]BF$_4$ and by the photochemical conversions of the *cis*-isomers in the presence of excess NH$_4$PF$_6$ (yield : 40–80%. The *trans*-isomers thermally isomerized back to the original *cis*-isomers with a very slow rate at room temperature. Such photochemical and thermal inter-conversions between two isomers have also been observed for other [Co(dtc)$_2$(phosphite or PHPh$_2$)$_2$]$^+$ complexes,[5,9] while no isomerization reaction was observed for tertiary phosphine complexes such as [Co(dtc)$_2$(PMe$_{3-n}$Ph$_n$)$_2$]$^+$ (n = 0–3).[8] As noted in the section on kinetic studies, the substituents on phosphorus play a critical role in the isomerization process. The quantum yields, Φ, for the photochemical isomerization of *cis*-[Co(dtc)$_2${P(OMe)Ph$_2$ or P(OMe)$_2$Ph}$_2$]$^+$ were 0.17–0.20 upon irradiation at 405 nm, which is comparable to that for the corresponding P(OCH$_2$)$_3$CEt complex (Φ = 0.17).[5]

Crystal structures

In the crystals of *trans*-[Co(dtc)$_2${P(OMe)$_3$}$_2$]BF$_4$ and *trans*-[Co(dtc)$_2${P(OMe)$_2$Ph}$_2$]BF$_4$·(CH$_3$)$_2$CO, two Co atoms, Co(1) and Co(2), were located at a crystallographic center of symmetry and the asymmetric unit contains two halves of the complex cation and a whole BF$_4^-$ anion (and an acetone molecule). The molecular structures of one of the two independent complex cations of *trans*-[Co(dtc)$_2${P(OMe)$_3$}$_2$]$^+$ and *trans*-[Co(dtc)$_2$-{P(OMe)$_2$Ph}$_2$]$^+$ are shown in Figs. 1a and 1b, respectively. The other complex cations exhibited similar structures to these with different orientations and conformations of the OMe and Ph substituents on the P atoms (see Figs. S1 and S2 †). For the *trans*-[Co(dtc)$_2${P(OMe)Ph$_2$}$_2$]BF$_4$·0.5CH$_3$OH complex, it was found that there were three positions for the Co atoms: Co(1) at a general position and Co(51) and Co(52) at a crystallographic center of symmetry. Thus, the asymmetric unit consists of one whole and two half complex cations, two BF$_4^-$ anions and a methanol molecule. The molecular structures of the three crystallographically independent complex cations were different in the orientation of the phenyl rings of P(OMe)Ph$_2$ (Fig. S3 †). In complex 1 with Co(1) at a general position, two crystallographically independent P(OMe)Ph$_2$ ligands exhibited orientation of their phenyl rings as found in either complex 51 or complex 52 (Fig. 1c and Table 3).

The structures of the Co(dtc)$_2$ moiety in *trans*-[Co(dtc)$_2$-{P(OMe)$_{3-n}$Ph$_n$}$_2$]$^+$ are similar to those found in the previously reported *trans*-[Co(dtc)$_2$(PMe$_{3-n}$Ph$_n$ or PHPh$_2$)$_2$]$^+$ complexes:[8,9] the Co–S bond lengths and the S–Co–S bite angles of dtc$^-$ are in the range of 2.264–2.278 Å and 76.0–77.0°, respectively (Table 4).

It is known that the Co–P bonds in *trans*-[Co^{III}(bidentate monoanionic ligand)$_2$(P-ligand)$_2$]$^+$ complexes are often elongated by steric interactions (the mutual steric *trans* influence) with the bidentate ligands in the equatorial plane: pentane-2,4-dionate (acac$^-$)[23] and dimethylglyoximate (Hdmg$^-$)[24] complexes are included in this type of complex. However, such a mutual steric *trans* influence does not seem to exist in the complexes with dtc$^-$ as the bidentate monoanionic ligand. This is probably caused by the small bulk of the dtc$^-$ ligand compared with acac$^-$ and Hdmg$^-$,[8] in addition to the electron sponge action of dtc$^-$ as described in the latter section. The average Co–P bond lengths in the *trans*-[Co(dtc)$_2$(P-ligand)$_2$]$^+$ complexes are summarized in Table 4, and the plots of Co–P length against the Tolman's cone angle[15] of each P-ligand is shown in Fig. 2, which clearly indicates that there is a linear relationship between the cone angle and the Co–P bond length for the series of *trans*-[Co(dtc)$_2$(P-ligand)]$^+$ complexes. As the σ-donicity for P(OMe)$_3$, P(OMe)$_2$Ph, P(OMe)Ph$_2$ and PPh$_3$ is unequivocally low and does not differ greatly from ligand to ligand (χ_d =

Table 2 Crystallographic data

Complex	*cis*-[Co(dtc)$_2${P(OMe)$_3$}$_2$]-BF$_4$	*cis*-[Co(dtc)$_2${P(OMe)$_2$Ph}$_2$]PF$_6$	*cis*-[Co(dtc)$_2${P(OMe)Ph$_2$}$_2$]PF$_6$	*trans*-[Co(dtc)$_2$-{P(OMe)$_3$}$_2$]BF$_4$	*trans*-[Co(dtc)$_2${P(OMe)$_2$Ph}$_2$]-BF$_4$·(CH$_3$)$_2$CO	2 × [*trans*-[Co(dtc)$_2${P(OMe)Ph$_2$}$_2$]-BF$_4$·0.5CH$_3$OH[a]
Chemical formula	$C_{12}H_{30}BCoF_4N_2O_6P_2S_4$	$C_{22}H_{34}CoF_6N_2O_4P_3S_4$	$C_{32}H_{38}CoF_6N_2O_2P_3S_4$	$C_{12}H_{30}BCoF_4N_2O_6P_2S_4$	$C_{25}H_{40}BCoF_4N_2O_5P_2S_4$	$C_{65}H_{80}B_2Co_2F_8N_4O_5P_4S_8$
Formula weight	634.30	784.59	876.72	634.30	784.51	834.59 × 2
Color and shape of crystal	Red, column	Red-orange, prism	Red, prism	Red, prism	Red, prism	Red, plate
Crystal system	Monoclinic	Monoclinic	Orthorhombic	Triclinic	Monoclinic	Triclinic
Space group	$P2_1/n$	$P2_1/c$	*Pbca*	$P\bar{1}$	$P2_1/a$	$P\bar{1}$
a/Å	7.323(4)	11.732(3)	18.893(6)	11.170(2)	11.025(2)	9.6508(5)
b/Å	13.349(3)	19.827(5)	25.288(3)	12.212(2)	12.594(2)	10.9697(8)
c/Å	26.733(3)	14.553(3)	16.688(2)	12.319(2)	25.581(2)	37.114(3)
α/°	90	90	90	109.67(2)	90	88.261(8)
β/°	95.56(2)	94.91(2)	90 109.07(1)	94.41(1)	84.228(7)	
γ/°	90	90	90	107.36(2)	90	85.066(8)
U/Å^3	2601(2)	3373(1)	7973(3)	1328.7(4)	3541.5(8)	3893.8(5)
Z	4	4	8	2	4	2
D_{calc}/Mg m^{-3}	1.620	1.545	1.461	1.585	1.471	1.424
F(000)	1304	1608	3600	652	1624	1724
μ(Mo-K$_\alpha$)/mm^{-1}	1.163	0.963	0.820	1.138	0.868	0.790
R_{int}	0.041	0.107	0.027	0.020	0.018	0.039
No. of independent reflections	7587	7728	11635	10336	10336	12588
*R*1 (F^2: $F_o^2 > 2\sigma(F_o^2)$)	0.044	0.057	0.047	0.054	0.045	0.093
*wR*2 (F^2: all data)	0.134	0.132	0.161	0.199	0.188	0.188

[a] Two *trans*-[Co(dtc)$_2${P(OMe)Ph$_2$}$_2$]BF$_4$in the unit cell.

Table 3 Selected bond lengths (Å) and angles (°) for the *trans*- and *cis*-$[Co(dtc)_2\{P(OMe)_{3-n}Ph_n\}_2]^+$ complexes

trans-isomers				*cis*-isomers			
trans-$[Co(dtc)_2\{P(OMe)_3\}_2]BF_4$				*cis*-$[Co(dtc)_2\{P(OMe)_3\}_2]BF_4$			
Co(1)–P(1)	2.239(1)	Co(2)–P(2)	2.243(1)	Co–P(1)	2.200(1)	Co–P(2)	2.200(1)
Co(1)–S(1)	2.273(1)	Co(2)–S(3)	2.265(1)	Co–S(1)	2.275(2)	Co–S(3)	2.266(2)
Co(1)–S(2)	2.274(1)	Co(2)–S(4)	2.280(1)	Co–S(2)	2.294(1)	Co–S(4)	2.297(1)
S(1)–Co(1)–S(2)	76.42(4)	S(3)–Co(2)–S(4)	76.76(5)	P(1)–Co(1)–P(2)	97.16(4)		
				S(1)–Co(1)–S(2)	75.59(4)	S(3)–Co(1)–S(4)	75.96(4)
trans-$[Co(dtc)_2\{P(OMe)_2Ph\}_2]BF_4\cdot(CH_3)_2CO$				*cis*-$[Co(dtc)_2\{P(OMe)_2Ph\}_2]PF_6$			
Co(1)–P(1)	2.263(2)	Co(2)–P(2)	2.269(1)	Co–P(1)	2.222(3)	Co–P(2)	2.214(3)
Co(1)–S(1)	2.259(1)	Co(2)–S(3)	2.268(1)	Co–S(1)	2.260(2)	Co–S(3)	2.265(2)
Co(1)–S(2)	2.268(1)	Co(2)–S(4)	2.265(1)	Co–S(2)	2.285(2)	Co–S(4)	2.293(3)
S(1)–Co(1)–S(2)	76.89(5)	S(3)–Co(2)–S(4)	76.99(5)	S(1)–Co(1)–S(2)	76.53(8)	S(3)–Co(1)–S(4)	76.35(9)
ϕ_1 [a]	28.5(1)	ϕ_2 [b]	26.8(2)	P(1)–Co(1)–P(2)	94.4(1)		
trans-$[Co(dtc)_2\{P(OMe)Ph_2\}_2]BF_4\cdot0.5CH_3OH$				*cis*-$[Co(dtc)_2\{P(OMe)Ph_2\}_2]PF_6$			
Co(1)–P(1)	2.269(2)	Co(1)–P(2)	2.309(2)	Co–P(1)	2.244(1)	Co–P(2)	2.246(1)
Co(1)–S(1)	2.279(2)	Co(1)–S(3)	2.281(2)	Co–S(1)	2.270(1)	Co–S(3)	2.271(1)
Co(1)–S(2)	2.280(2)	Co(1)–S(4)	2.275(2)	Co–S(2)	2.288(1)	Co–S(4)	2.297(1)
P(1)–Co(1)–P(2)	173.71(7)						
S(1)–Co(1)–S(2)	76.23(7)	S(3)–Co(1)–S(4)	76.48(7)	P(1)–Co(1)–P(2)	92.68(4)		
S(1)–Co(1)–S(4)	99.96(7)	S(2)–Co(1)–S(3)	107.42(7)	S(1)–Co(1)–S(2)	76.13(4)	S(3)–Co(1)–S(4)	75.73(4)
ϕ_1 [c]	25.8(2)	ϕ_3 [c]	26.2(3)				
ϕ_2 [c]	89.2(2)	ϕ_4 [c]	18.6(2)				
Co(51)–P(51)	2.285(2)	Co(52)–P(52)	2.301(2)				
Co(51)–S(51)	2.285(2)	Co(52)–S(53)	2.270(2)				
Co(51)–S(52)	2.280(2)	Co(52)–S(54)	2.271(2)				
S(51)–Co(51)–S(52)	76.08(6)	S(53)–Co(52)–S(54)	76.90(6)				
ϕ_{51} [d]	21.1(2)	ϕ_{53} [e]	21.0(2)				
ϕ_{52} [d]	89.0(2)	ϕ_{54} [e]	31.6(3)				

[a] Dihedral angle between the $CoS_4(1)$ plane (defined by Co(1), S(1) and S(2)) and the phenyl ring consisted of C(11)–C(16). [b] Dihedral angle between the $CoS_4(2)$ plane (defined by Co(2), S(3) and S(4)) and the phenyl ring consisted of C(31)–C(36). [c] Dihedral angle between the $Co(1)S_4$ plane (defined by Co(1), S(1), S(2), S(3) and S(4)) and the four phenyl rings of complex 1: phenyl(1) C(11)–C(16); phenyl(2) C(17)–C(22); phenyl(3) C(31)–C(36); phenyl(4) C(37)–C(42). [d] Dihedral angle between the $Co(51)S_4$ plane (defined by Co(51), S(51) and S(52)) and the two crystallographically independent phenyl rings of complex 51: phenyl(51) C(61)–C(66); phenyl(52) C(67)–C(72). [e] Dihedral angle between the $Co(52)S_4$ plane (defined by Co(52), S(53) and S(54)) and the two crystallographically independent phenyl rings of complex 52: phenyl(53) C(81)–C(86); phenyl(54) C(87)–C(92).

Table 4 Structural and electronic parameters for P-ligands and average bond lengths (Å) and angles (°) in *trans*- and *cis*-$[Co(dtc)_2(P\text{-ligand})_2]^+$ complexes

				trans-$[Co(dtc)_2(P\text{-ligand})_2]^+$			*cis*-$[Co(dtc)_2(P\text{-ligand})_2]^+$				
P-ligand	θ_T [a]	χ [b]	χ_d [b]	Co–P	Co–S	S–Co–S	Co–P	Co–S(*trans*S)	Co–S(*trans*P)	P–Co–P	S–Co–S
$P(OMe)_3$	107	24.10	16.70	2.241	2.273	76.25	2.200	2.270	2.295	97.16	75.78
$P(OMe)_2Ph$	115	19.45	15.73	2.266	2.265	76.91	2.218	2.263	2.289	94.4	76.44
$P(OMe)Ph_2$	132	16.30	14.82	2.291	2.277	76.42	2.245	2.271	2.292	92.68	75.93
PPh_3	145	13.25	13.25	2.316	2.264	76.2	–				
$PMePh_2$	136	12.10	12.10	2.303	2.278	76.18	–				
PMe_2Ph	122	10.60	10.60	2.284	2.270	76.75	2.272	2.268	2.291	95.14	76.31
PMe_3	118	8.55	8.55	2.287	2.270	76.86	2.200	2.255	2.310	96.8	75.07
$PHPh_2$	128	17.35	17.35	2.276	2.269	77.03	2.230	2.263	2.283	90.51	76.52

[a] Tolman's cone angle from ref. 15. [b] From ref. 10.

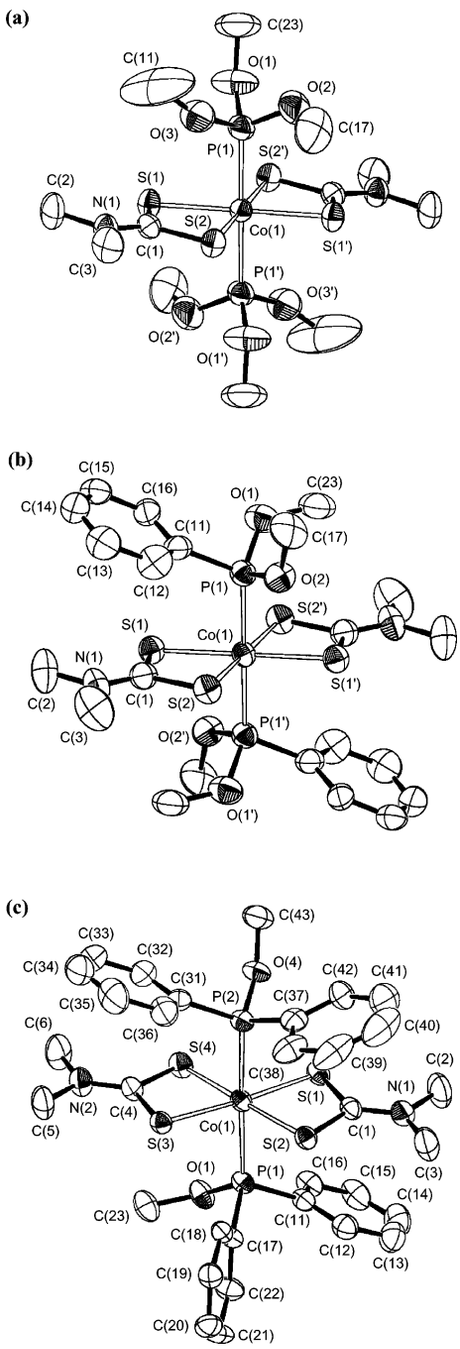

Fig. 1 Perspective views of one of the crystallographically independent complex cations in (a) *trans*-$[Co(dtc)_2\{P(OMe)_3\}_2]BF_4$ (40% probability level), (b) *trans*-$[Co(dtc)_2\{P(OMe)_2Ph\}_2]BF_4 \cdot (CH_3)_2CO$ (50% probability level) and (c) *trans*-$[Co(dtc)_2\{P(OMe)Ph_2\}_2]BF_4 \cdot 0.5CH_3OH$ (40% probability level). Hydrogen atoms are omitted for clarity.

16.70–13.25), the linear relation in Fig. 2 indicates that the Co–P bond lengths depend primarily on the steric requirements (Tolman's cone angle, θ_T) of the P-ligands. The fact that a very weak σ-donor, $PHPh_2$, is also located on the same straight line in Fig. 2 confirms the validity of the above assertion. On the other hand, when the P-ligand is either PMe_3 or PMe_2Ph, the Co–P bond length is longer than that predicted from the straight line in Fig. 2. We presume that this deviation is the net elongation caused by the electronic mutual *trans* influence. Therefore, we conclude that the electronic *trans* influence of the P-ligand, that seems to be parallel to the σ-donicity of the P-ligand, is the secondary factor that determines the Co–P bond lengths in the series of *trans*-$[Co(dtc)_2(P\text{-ligand})_2]^+$ complexes: the primary factor to govern the bond lengths is the cone angle of each ligand.

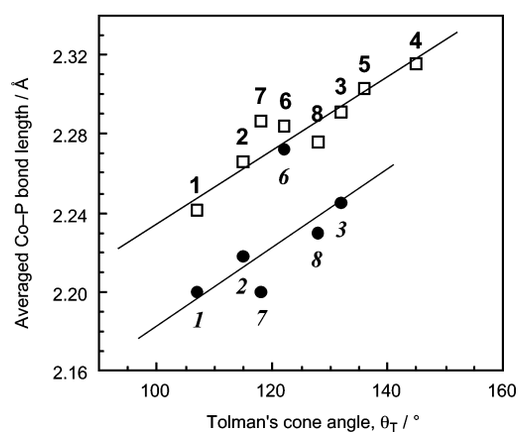

Fig. 2 Plots of the Co–P bond lengths (Å) against the Tolman's cone angle of the P-ligands in *trans*- and *cis*-$[Co(dtc)_2(P\text{-ligand})_2]^+$ (□: *trans* complex, ●: *cis* complex). P-ligand = 1: $P(OMe)_3$, 2: $P(OMe)_2Ph$, 3: $P(OMe)Ph_2$, 4: PPh_3, 5: $PMePh_2$, 6: PMe_2Ph, 7: PMe_3, 8: $PHPh_2$.

The structures of *cis*-$[Co(dtc)_2\{P(OMe)_{3-n}Ph_n\}_2]^+$ (n = 0, 1 or 2) are shown in Fig. 3, and the structural parameters are listed in Table 3. The Co–S bond lengths *trans* to the P-ligand are longer by 0.02–0.03 Å than those for the mutually *trans* Co–S (Table 4). Such a tendency was also common in the other *cis*-$[Co(dtc)_2(P\text{-ligand})_2]^+$ complexes.[5,8,9] The small elongation of the Co–S bond may be attributed to the larger *trans* influence of the P-ligand compared with that of dtc^-. Moreover, the elongations of the Co–S bonds *trans* to the P-ligands in the bis(dtc) complexes are smaller than those observed for the Co–O bonds at the *trans* position of the P-ligands in *cis*-$[Co(acac)_2(P\text{-ligand})_2]^+$ complexes,[25,26] indicating the larger electron sponge effect of dtc^- compared with $acac^-$. The Co–P bonds in *cis*-$[Co(dtc)_2\{P(OMe)_{3-n}Ph_n\}_2]^+$ were shorter by 0.04–0.05 Å than those in the corresponding *trans*-isomers, which is due to a combination of the reduced *trans* influence, the reduced steric congestion around the Co–P bond, and the electron-buffer effect by the dtc^- ligand in the *cis*-complexes.

Table 5 Results of the Gaussian curve fitting for the absorption band maxima, $10^{-3}\sigma/cm^{-1}$ ($\varepsilon/dm^3\ mol^{-3}\ cm^{-1}$),[a] of $[Co(dtc)_2(P\text{-ligand})_2]^+$ complexes

Complex	d–d band	CT band
$[Co(dtc)_3]$	15.50 (435), 20.62 (589)	25.87 (8437), 27.73 (2794), 31.21 (19490)
cis-$[Co(dtc)_2\{P(OMe)_3\}_2]BF_4$	19.41 (704), 23.73 (1552)	29.03 (9840), 34.08 (26980), 39.32 (19530)
cis-$[Co(dtc)_2\{P(OMe)_2Ph\}_2]PF_6$	19.12 (714), 23.45 (1947)	28.64 (10430), 32.25 (10810), 35.88 (28540)
cis-$[Co(dtc)_2\{P(OMe)Ph_2\}_2]PF_6$	18.33 (691), 23.20 (2382)	28.43 (10820), 31.33 (11000), 35.27 (27990)
cis-$[Co(dtc)_2(PMe_2Ph)_2]PF_6$	17.91 (743), 22.96 (1716)	28.89 (15200), 32.04 (21800)
cis-$[Co(dtc)_2(PMe_3)_2]BF_4$	18.33 (741), 23.31 (1340)	29.25 (10560), 32.62 (24990)
cis-$[Co(dtc)_2(PHPh_2)_2]BF_4$	18.43 (654), 23.43 (2611)	27.89 (5354), 31.17 (7791), 34.59 (26770)
trans-$[Co(dtc)_2\{P(OMe)_3\}_2]BF_4$	20.23 (415)	27.76 (9477), 29.59 (13120), 33.15 (10800)
trans-$[Co(dtc)_2\{P(OMe)_2Ph\}_2]BF_4$	18.20 (335)	26.42 (9743), 29.15 (16100), 31.91 (12160)
trans-$[Co(dtc)_2\{P(OMe)Ph_2\}_2]BF_4$	17.66 (448)	25.04 (8615), 28.47 (10220), 30.94 (17240)
trans-$[Co(dtc)_2(PPh_3)_2]BF_4$	15.74 (342)	23.08 (9488), 30.18 (22290)
trans-$[Co(dtc)_2(PMePh_2)_2]BF_4$	16.58 (355), 19.97 (581)	24.77 (10950), 29.63 (21750)
trans-$[Co(dtc)_2(PMe_2Ph)_2]BF_4$	17.17 (225)	25.57 (12090), 29.70 (25120)
trans-$[Co(dtc)_2(PMe_3)_2]BF_4$	17.90 (258)	27.38 (13540), 30.11 (21970)
trans-$[Co(dtc)_2(PHPh_2)_2]BF_4$	17.30 (369), 21.12 (617)	24.92 (10910), 29.63 (21130)

[a] In dichloromethane at room temperature.

As shown in Fig. 2, the relation between the Co–P bond length and θ_T for the *cis* complexes is somewhat dispersed but almost linear. However, there is no apparent relationship between the P–Co–P bond angle and θ_T for the *cis*-complexes as seen in Table 4: it seems that the electron sponge effect of dtc^- causes alteration of the P–Co–P angle as described in the latter section, although it is also possible to consider that a suitable orientation of the substituents on the P atom in the crystal alters the configuration around the cobalt center.[27]

Absorption spectra

The UV-Vis absorption spectra of *cis*- and *trans*-$[Co(dtc)_2\{P(OMe)_{3-n}Ph_n\}_2]^+$ complexes in dichloromethane are shown in Fig. 4, which are similar to those for the analogous *cis*- and *trans*-$[Co(dtc)_2(PMe_{3-n}Ph_n)_2]^+$ complexes.[8] For the *cis*-complexes (Fig. 4a), there exists a weak ($\varepsilon < 750\ dm^3\ mol^{-1}\ cm^{-1}$) shoulder around 19000 cm^{-1} and an absorption band ($\varepsilon < 2500\ dm^3\ mol^{-1}\ cm^{-1}$) around 23500 cm^{-1}, that were assigned to the first ($^1A_{1g} \longrightarrow {}^1T_{1g}$: O_h) and the second ($^1A_{1g} \longrightarrow {}^1T_{2g}$) d–d transition bands, respectively.[8] The distinct splitting of the d–d band due to the low molecular symmetry, C_2 (or holohedrized D_{4h}) was not observed, as was the case for the other analogous P-ligand complexes.[5,8,9] The peak positions of these transition bands estimated by the Gaussian curve fitting analyses are listed in Table 5, from which the ligand-field strength, Δ, and the Racah's inter-electronic repulsion parameter, *B*, were estimated by assuming $C = 4B$: $\Delta = 20490\ cm^{-1}$ and $B = 270\ cm^{-1}$ for *cis*-$[Co(dtc)_2\{P(OMe)_3\}_2]^+$, $\Delta = 20200\ cm^{-1}$ and $B = 271\ cm^{-1}$ for *cis*-$[Co(dtc)_2\{P(OMe)_2Ph\}_2]^+$, and $\Delta = 19550\ cm^{-1}$ and $B = 304\ cm^{-1}$ for *cis*-$[Co(dtc)_2\{P(OMe)Ph_2\}_2]^+$. It should be noted that the ligand-field strength gets larger in the order $P(OMe)Ph_2 < P(OMe)_2Ph < P(OMe)_3$ of these P-ligands, while the σ-donicity of these P-ligands slightly decreases in this order, indicative of the importance of π-back bonding between Co(III) and P-ligands: the π-acidity of the P-ligand increases in this order. The ligand-field strengths for the $P(OMe)_3$ and $P(OMe)_2Ph$ complexes are larger but the *B* parameters for these complexes are smaller than those for the PMe_3 ($\Delta = 19570$ and $B = 311\ cm^{-1}$) and PMe_2Ph ($\Delta = 19170$ and $B = 316\ cm^{-1}$) complexes.[8] The *cis*-complexes also exhibited two intense absorption bands in the UV region, which were assigned to ligand-to-metal charger transfer (LMCT) bands.

The absorption spectra of *trans*-$[Co(dtc)_2\{P(OMe)_{3-n}Ph_n\}_2]^+$ (Fig. 4b), exhibited only a weak ($\varepsilon < 500\ dm^3\ mol^{-1}\ cm^{-1}$) shoulder in the 17000–20000 cm^{-1} region, that was assigned to the splitting component ($^1A_{1g} \longrightarrow a^1E_g$: D_{4h}) of the first d–d transition. The *trans*-isomers also exhibited some intense bands at higher energy (> 23000–27000 cm^{-1}), that were assigned to the LMCT band in agreement with other related *trans*-complexes.[8,23]

It was expected that the $^1A_{1g} \longrightarrow a^1E_g$ transition energy, that is parallel to the ligand-field strength, is linearly related to Tolman's χ parameter, as this parameter includes the effect of π-acceptability. As seen from Fig. 5a, however, a V-shaped relation was found in such a plot for the series of *trans*-complexes. A similar tendency was also found for the series of *cis*-complexes. Such a V-shaped relation indicates that Tolman's χ parameter fails to predict the exact nature of the σ and π-back bonding interactions between cobalt(III) and these P-ligands. However, it is more rational to conclude that the steric factor represented by the cone angle overrules the contribution of the electronic factors represented by Tolman's χ parameter (Fig. 5b). A similar conclusion was also derived for the *trans* influence (Fig. 2): the σ-donicity (= electronic factor) of the P-ligand is the secondary factor that determines the Co–P bond lengths in the *trans*-$[Co(dtc)_2(P\text{-ligand})_2]^+$ complexes, while the primary factor to govern the bond lengths is the cone angle of each P-ligand.

Isomerization reactions

NMR measurements. The observed ^1H NMR spectral changes are shown in Fig. 6 for the *trans* to *cis* isomerization reaction of $[Co(dtc)_2\{P(OMe)Ph_2\}_2]^+$ (0.01 mol kg^{-1}) in acetonitrile at 303 K. It is shown that the proton signals corresponding to the *trans*-species decreased with time while the signals corresponding to the *cis*-species increased. Although the low sensitivity of the NMR method did not allow us to observe decomposition products during the experiment, it was shown that a small amount of gradual decomposition did take place causing a slight deviation in the spectral intensity with time from the first-order kinetics, when no free $P(OMe)Ph_2$ was added to the reaction mixture. A slow decomposition of the complex was also indicated for the isomerization reaction of *trans*-$[Co(dtc)_2\{P(OMe)_2Ph\}_2]^+$ in the absence of free $P(OMe)_2Ph$.

On the other hand, the ^1H NMR spectral changes for the isomerization reaction of *trans*-$[Co(dtc)_2\{P(OMe)_3\}_2]^+$ were somewhat different from those for the other two complexes. In addition to the deviation from the first-order kinetics, the NMR signals that indicate decomposition and/or intramolecular isomerization of the free $P(OMe)_3$ ligand were observed when an excess amount of free $P(OMe)_3$ was added to the solution: the solution without free $P(OMe)_3$ exhibited complicated NMR signals with time, indicating gradual decomposition of the compound in a complex manner. Fig. 7 shows the ^1H NMR spectrum of a sample solution containing $[Co(dtc)_2\{P(OMe)_3\}_2]^+$ (0.01 mol kg^{-1}) with an excess (*ca.* 4 times more than the complex) amount of free $P(OMe)_3$. This spectrum was observed after completion of the isomerization reaction at 303 K. The $N–CH_3$ and $P–OCH_3$ signals in the figure are those

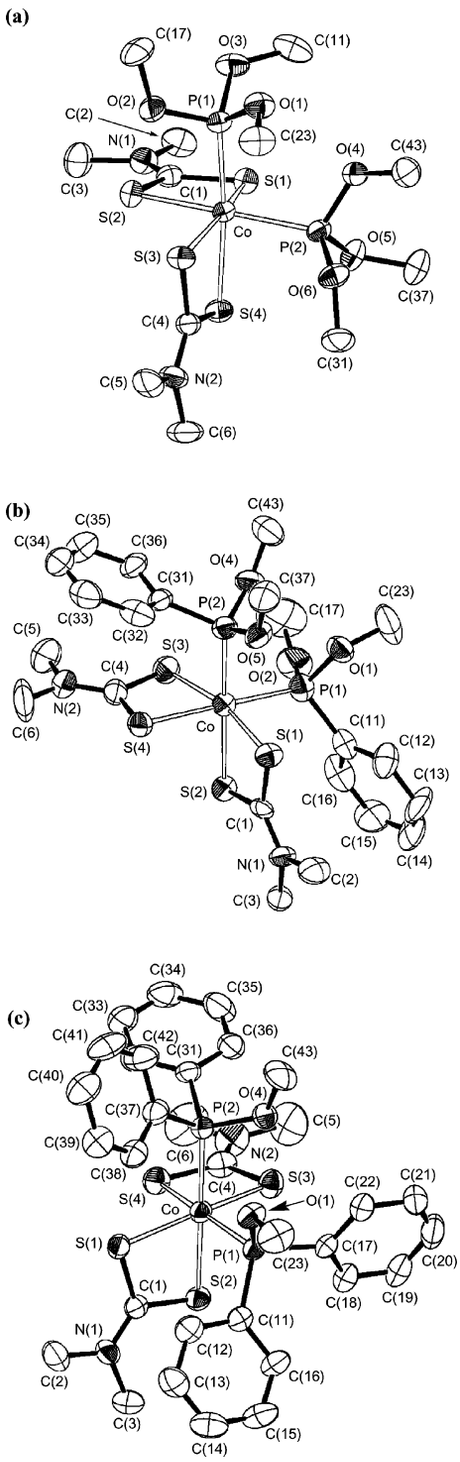

Fig. 3 Perspective views (40% probability level for each crystal) of the cationic part in (a) *cis*-$[Co(dtc)_2\{P(OMe)_3\}_2]BF_4$, (b) *cis*-$[Co(dtc)_2\{P(OMe)_2Ph\}_2]PF_6$ and (c) *cis*-$[Co(dtc)_2\{P(OMe)Ph_2\}_2]PF_6$. Hydrogen atoms are omitted for clarity.

for the *cis*-isomers. Beside the doublet signals for free $P(OMe)_3$, small signals located at 3.71, 5.80, and 7.55 ppm and a series of signals at 3.28 and around 3.68 ppm were observed. The latter two signals, exhibiting a 12 : 9 ratio in terms of the proton numbers, were assigned to the $N–CH_3$ and $P–OCH_3$ protons in the 5-coordinate $[Co(dtc)_2\{P(OMe)_3\}]^+$ species (the validity of this assignment is shown in the latter section), while the other signals correspond to the decomposition products of $P(OMe)_3$ in the bulk: it is known that free $P(OMe)_3$ tends to either isomerize to $P(=O)(Me)(OMe)_2$ or decompose to produce a series of $HPMe_x(O)(OMe)_y$[28] and the latter species exhibits ^1H NMR signals in this region.[29] It seems that the coordinated $P(OMe)_3$ is

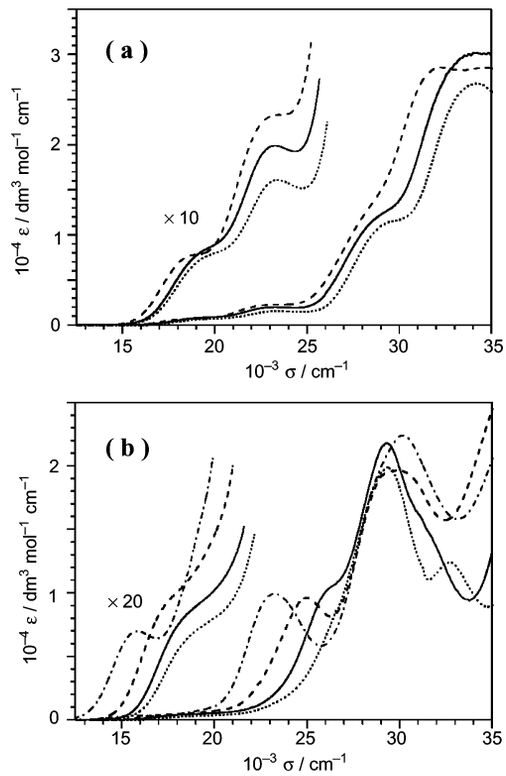

Fig. 4 UV-Vis absorption spectra of (a) *cis*- and (b) *trans*-$[Co(dtc)_2\{P(OMe)_{3-n}Ph_n\}_2]^+$ (n = 0 (···); 1 (—); 2 (---) and 3 (-·-)) in dichloromethane at room temperature.

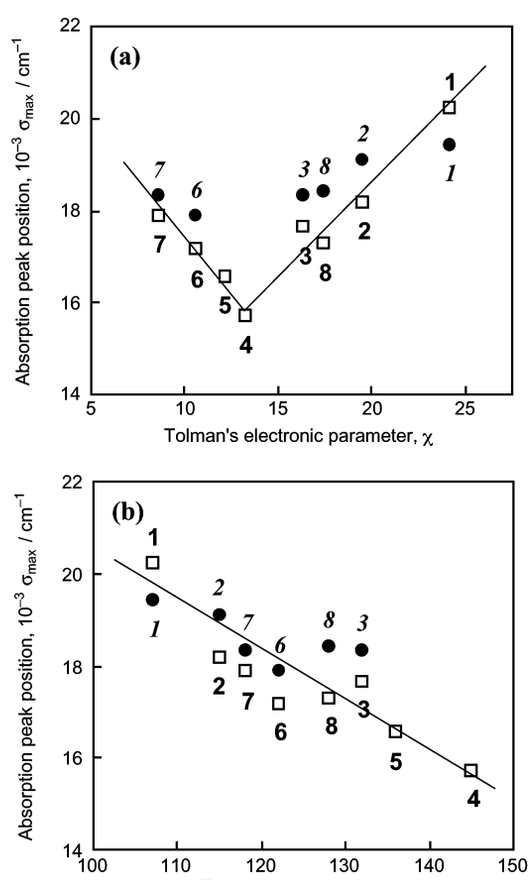

Fig. 5 Plots of the d–d band positions (σ/cm^{-1}) against (a) Tolman's electronic parameter (χ) and (b) Tolman's cone angle (θ_T/°) for the P-ligands in *trans*- and *cis*-$[Co(dtc)_2(P\text{-ligand})_2]^+$. □ : d–d ($a^1E_g$) band of the *trans*-isomers; ● : d–d ($^1T_{1g}$: O_h) band of the *cis*-isomers. P-ligand = 1: $P(OMe)_3$, 2: $P(OMe)_2Ph$, 3: $P(OMe)Ph_2$, 4: PPh_3, 5: $PMePh_2$, 6: PMe_2Ph, 7: PMe_3, 8: $PHPh_2$.

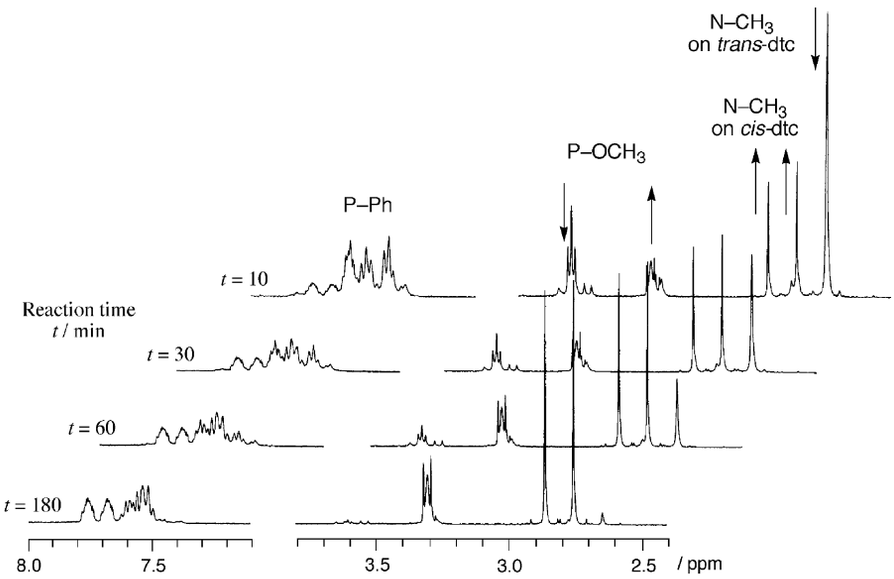

Fig. 6 ^{1}H NMR spectral change for *trans* to *cis* thermal isomerization reaction of $[Co(dtc)_2\{P(OMe)Ph_2\}_2]^+$ at 303 K in acetonitrile-d_3. [*trans*-$Co(dtc)_2\{P(OMe)Ph_2\}^{2+}]_0$ = 0.01 mol kg^{-1}. CF_3SO_3Na (0.1 mol kg^{-1}) was used as the supporting electrolyte.

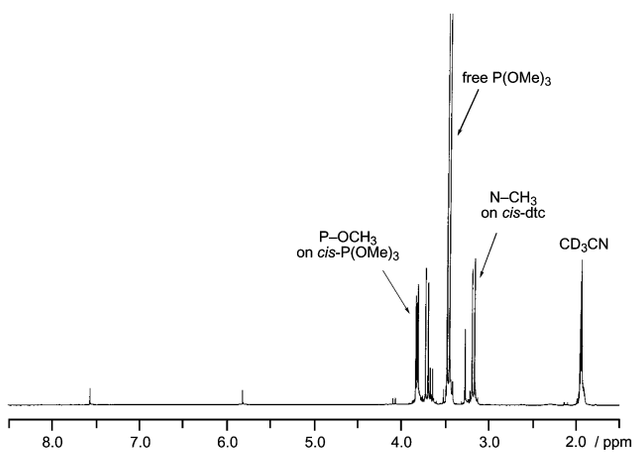

Fig. 7 ^{1}H NMR spectrum after completion of the thermal *trans* to *cis* isomerization reaction of $[Co(dtc)_2\{P(OMe)_3\}_2]^+$ with excess free $P(OMe)_3$ at 303 K in acetonitrile-d_3. [*trans*-$Co(dtc)_2\{P(OMe)_3\}^{2+}]_0$ = 0.01 mol kg^{-1}. The concentration of free $P(OMe)_3$ in the bulk is *ca*. 0.04 mol kg^{-1}. CF_3SO_3Na (0.1 mol kg^{-1}) was used as the supporting electrolyte.

not subject to the intramolecular isomerization to P(=O)(Me)-$(OMe)_2$ and/or decomposition, while the sample solution containing only $P(OMe)_3$ exhibited similar NMR signals to those in Fig. 7 after several hours: a similar difference in the reactivity of the coordinated and free phosphine ligand was observed for the isomerization reaction of the $PHPh_2$ complex in a previous study[9a] where impure water abstracts the P–H proton from free $PHPh_2$ but not from coordinated $PHPh_2$. It seems, therefore, that an acid–base interaction between free $P(OMe)_3$ and impure water (*ca*. 1 mmol kg^{-1}) provides a variety of decomposition processes for free $P(OMe)_3$. Otherwise, the excess amount of added free $P(OMe)_3$ (> *ca*. 5 mmol) significantly suppresses unfavorable side reactions initiated by the dissociation of coordinated $P(OMe)_3$.

Spectrophotometric measurements

As shown in Fig. 8a, although *trans*-$[Co(dtc)_2\{P(OMe)Ph_2\}_2]^+$ and *trans*-$[Co(dtc)_2\{P(OMe)_2Ph\}_2]^+$ undergo thermal isomerization to the corresponding *cis*-isomers, it was not possible to describe the change in the absorption with time by simple first-order kinetics. However, by addition of excess free ligand ($P(OMe)Ph_2$ or $P(OMe)_2Ph$), the reaction traces obeyed simple first-order kinetics (Fig. 8b) for up to three half-lives.

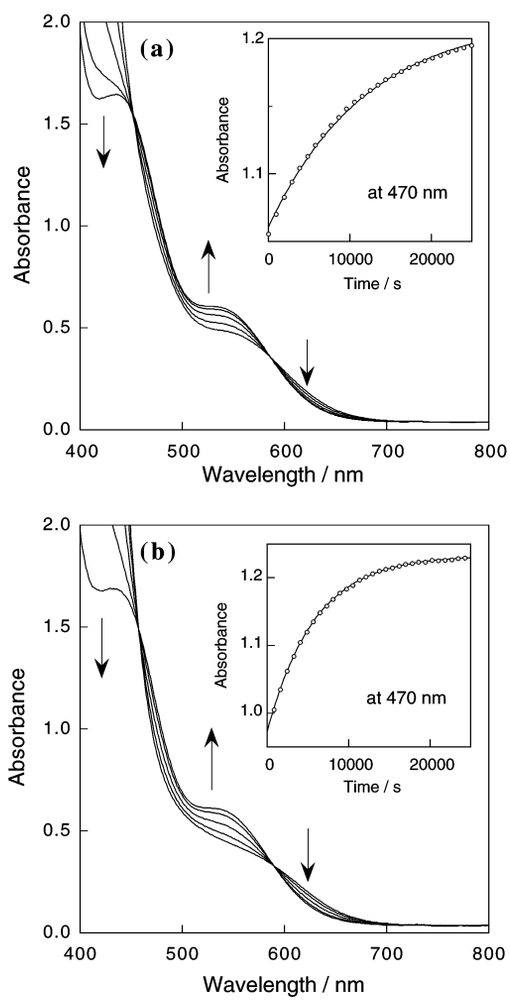

Fig. 8 Absorption spectral change for the thermal *trans* to *cis* isomerization reaction of $[Co(dtc)_2\{P(OMe)Ph_2\}_2]^+$ at 298 K in acetonitrile (a) without and (b) with excess free $P(OMe)Ph_2$ in the bulk. The inset in each figure shows the observed absorbance change with time at 470 nm and the corresponding best-fit curve analyzed by the single-exponential function.

The observed first-order rate constants were independent of the concentration of free ligand (Table 6). On the other hand, the dependence of the conditional first-order rate constants on

the concentration of excess free $P(OMe)_3$ exhibited saturation kinetics as shown in Fig. 9, while the absorption change with time for each given $[P(OMe)_3]_{free}$ was excellently first-order for up to 3 half-lives. It seems obvious that the degree of dissociation of coordinated $P(OMe)_3$ is large for *trans*-$[Co(dtc)_2\{P(OMe)_3\}_2]^+$ in acetonitrile while such a tendency is small for the *trans*-$P(OMe)_2Ph$ and -$P(OMe)Ph_2$ complexes.

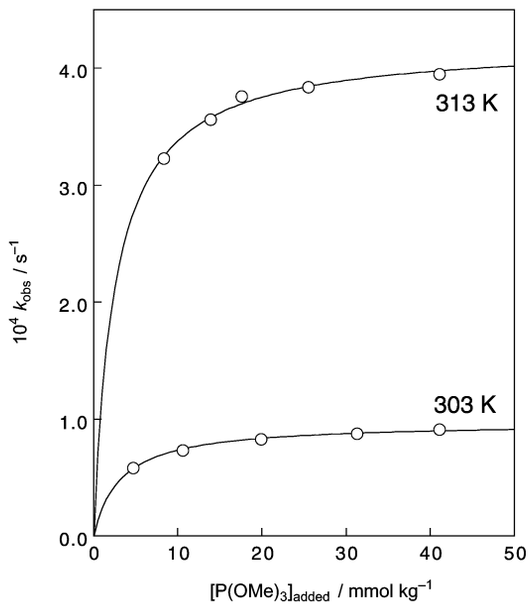

Fig. 9 The dependence of the conditional rate constants for the thermal *trans* to *cis* isomerization reaction of $[Co(dtc)_2\{P(OMe)_3\}_2]^+$ on the concentration of excess free $P(OMe)_3$ at 313 and 303 K. [*trans*-$Co(dtc)_2\{P(OMe)_3\}^{2+}]_0$ = 1.0 mmol kg^{-1}. Tetra-*n*-butylammonium tetrafluoroborate (0.1 mol kg^{-1}) was used as the supporting electrolyte.

Possible mechanisms for the *trans* to *cis* isomerization reactions are either (1) the dissociative mechanism through a 5-coordinate intermediate and (2) the intramolecular twist mechanism through the intermediate with trigonal-prismatic structure.[11] It was shown in a previous study,[9a] that the dissociative isomerization that takes place with the structural change from the square-pyramidal intermediate (A) (see Scheme 1) to the *cis*-product *via* the trigonal-bipyramidal transition state (B) cannot compete with the intramolecular twist mechanism because the structural change from (A) to (B) is accompanied by a very large activation enthalpy when the ligand-field is strong.[11–13] Therefore, although the overall reaction mechanism including dissociation of a coordinated P-ligand is expressed by the following equations, the k_2 process may only lead to decomposition of the 5-coordinate intermediate through further dissociation of the P-ligands that certainly explain the bi-exponential nature of the kinetic trace when no free ligand is added to the solution.

$$trans\text{-}[Co(dtc)_2(P\text{-ligand})_2]^+ \underset{k_{-1}}{\overset{k_1}{\rightleftharpoons}} trans\text{-}[Co(dtc)_2(P\text{-ligand})]^+(A) + P\text{-ligand} \quad (1)$$

$$trans\text{-}[Co(dtc)_2(P\text{-ligand})_2]^+(A) + P\text{-ligand} \xrightarrow{k_2} \text{transition state (B)} + P\text{-ligand} \longrightarrow \text{or further decomposition} \quad (2)$$

$$trans\text{-}[Co(dtc)_2(P\text{-ligand})_2]^+ \xrightarrow{k_3} cis\text{-}[Co(dtc)_2(P\text{-ligand})_2]^+ \quad (3)$$

By assuming a steady-state for the *trans*-$[Co(dtc)_2(P\text{-ligand})]^+$ (A) species, the following rate law is derived.

$$-\frac{d[trans\text{-}Co(dtc)_2(P\text{-ligand})_2^+]}{dt} = k_{obs}[trans\text{-}Co(dtc)_2(P\text{-ligand})_2^+]$$

$$k_{obs} = \frac{k_1k_2}{(k_{-1}[P\text{-ligand}]_{free} + k_2)} + k_3 \quad (4)$$

The k_{-1} process should be large when large amounts of free P-ligand exist in the solution. Therefore, eqn. (4) reduces to eqn. (5) under the experimental conditions.

$$k_{obs} = \frac{k_1k_2}{k_{-1}[P\text{-ligand}]_{free}} + k_3 \quad (5)$$

It is obvious, from Table 6, that the apparent rate constant for the *trans* to *cis* isomerization reaction is independent of the concentration of added free P-ligand, when $[P(OMe)_2Ph]_{free}$ or $[P(OMe)Ph_2]_{free}$ > 10 mmol kg^{-1}. Lack of the dependence of k_{obs} on $[P(OMe)_2Ph]_{free}$ or $[P(OMe)Ph_2]_{free}$ strongly indicates that the dissociation mechanism expressed by reactions (1) and (2) is not important when sufficient amounts of free $P(OMe)_2Ph$ or $P(OMe)Ph_2$ exist in the bulk. This result is also consistent with the NMR observation: there is no appreciable dissociation of coordinated $P(OMe)_2Ph$ or $P(OMe)Ph_2$.

The situation is somewhat different in the case of the isomerization reaction of *trans*-$[Co(dtc)_2\{P(OMe)_3\}_2]^+$. The dependence of the first-order rate constant on the concentration of free $P(OMe)_3$ exhibited saturation behavior (Fig. 9). Such a result is explained by assuming a *rapid equilibrium* for eqn. (1).[11]

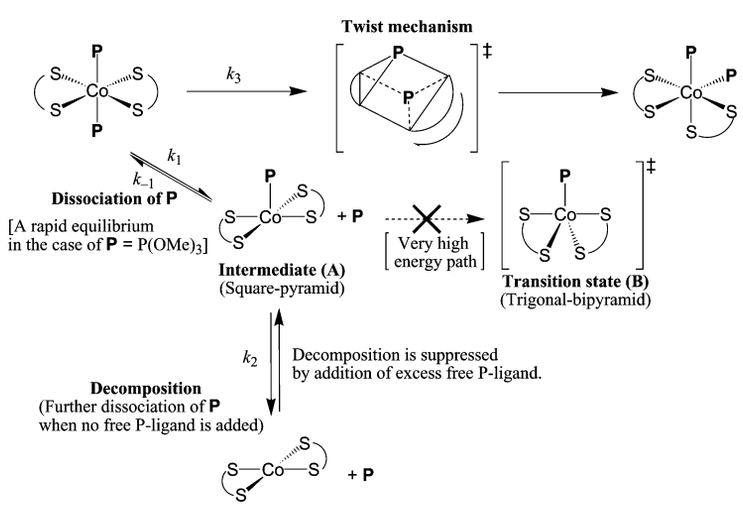

Scheme 1 Proposed mechanism for the thermal *trans* to *cis* isomerization reactions of $[Co(dtc)_2\{P(OMe)_{3-n}Ph_n\}_2]^+$.

Table 6 Kinetic data and parameters for the thermal *trans* to *cis* isomerization of $[Co(dtc)_2\{P(OMe)_{3-n}Ph_n\}_2]^+$ in acetonitrile[a]

$[Co(dtc)_2\{P(OMe)Ph_2\}_2]^+$			$[Co(dtc)_2\{P(OMe)_2Ph\}_2]^+$			$[Co(dtc)_2\{P(OMe)_3\}_2]^+$		
T/K[b]	$[P(OMe)Ph_2]_{free}$/mmol kg^{-1}	k_{obs}/s^{-1}	T/K[b]	$[P(OMe)_2Ph]_{free}$/mmol kg^{-1}	k_{obs}/s^{-1}	T/K[b]	$[P(OMe)_3]_{free}$/mmol kg^{-1}	k_{obs}/s^{-1}
293.1	41.4	$(8.33 \pm 0.04) \times 10^{-5}$	293.6	40.3	$(2.83 \pm 0.10) \times 10^{-6}$	293.1	40.8	$(1.77 \pm 0.01) \times 10^{-5}$
298.2	34.5	$(1.76 \pm 0.02) \times 10^{-4}$	298.7	40.3	$(6.57 \pm 0.08) \times 10^{-6}$	298.2	40.8	$(4.08 \pm 0.04) \times 10^{-5}$
303.2	44.1	$(3.52 \pm 0.09) \times 10^{-4}$	303.2	41.9	$(1.28 \pm 0.03) \times 10^{-5}$	303.1	41.1	$(9.12 \pm 0.06) \times 10^{-5}$
308.1	34.5	$(6.78 \pm 0.10) \times 10^{-4}$	308.2	40.3	$(2.34 \pm 0.02) \times 10^{-5}$	303.1	31.3	$(8.76 \pm 0.02) \times 10^{-5}$
313.2	44.1	$(1.42 \pm 0.04) \times 10^{-3}$	313.1	41.9	$(5.06 \pm 0.04) \times 10^{-5}$	303.1	19.9	$(8.27 \pm 0.08) \times 10^{-5}$
313.2	32.4	$(1.22 \pm 0.04) \times 10^{-3}$	313.1	26.4	$(5.52 \pm 0.08) \times 10^{-5}$	303.1	10.6	$(7.35 \pm 0.01) \times 10^{-5}$
313.2	25.9	$(1.29 \pm 0.04) \times 10^{-3}$	313.1	18.0	$(4.94 \pm 0.03) \times 10^{-5}$	303.1	4.70	$(5.85 \pm 0.01) \times 10^{-5}$
313.2	19.3	$(1.33 \pm 0.03) \times 10^{-3}$	313.1	12.4	$(5.62 \pm 0.08) \times 10^{-5}$	308.1	40.8	$(1.87 \pm 0.02) \times 10^{-4}$
313.2	15.8	$(1.38 \pm 0.03) \times 10^{-3}$	313.1	8.68	$(5.17 \pm 0.02) \times 10^{-5}$	313.2	41.1	$(3.95 \pm 0.02) \times 10^{-4}$
313.2	10.3	$(1.21 \pm 0.04) \times 10^{-3}$	313.1	6.90	$(5.25 \pm 0.03) \times 10^{-5}$	313.1	25.5	$(3.84 \pm 0.02) \times 10^{-4}$
						313.1	17.6	$(3.76 \pm 0.04) \times 10^{-4}$
						313.1	13.9	$(3.56 \pm 0.03) \times 10^{-4}$
						313.1	8.33	$(3.23 \pm 0.02) \times 10^{-4}$
$\Delta H^{\ddagger}$/kJ mol^{-1}		102 ± 2	$\Delta H^{\ddagger}$/kJ mol^{-1}		111 ± 3	$\Delta H^{\ddagger}$/kJ mol^{-1}[d]		115 ± 2
$\Delta S^{\ddagger}$/J mol^{-1} K^{-1}		24 ± 6	$\Delta S^{\ddagger}$/J mol^{-1} K^{-1}		28 ± 7	$\Delta S^{\ddagger}$/J mol^{-1} K^{-1}[d]		58 ± 4
k^{298}/s^{-1}[c]		1.5×10^{-4}	k^{298}/s^{-1}[c]		6.4×10^{-6}	k^{298}/s^{-1}[c,d]		4.1×10^{-5}[e]

[a] The concentration of $[Co(dtc)_2\{P(OMe)_{3-n}Ph_n\}_2]^+$ was adjusted to (1.00 ± 0.02) mmol kg^{-1} for all samples. Ionic strength of the solutions was adjusted to 0.1 mol kg^{-1} by using tetra-*n*-butylammonium tetrafluoroborate. [b] The temperature of all sample solutions was held constant within ± 0.2 K. [c] The rate constant at 25 °C was estimated from the activation parameters. [d] The kinetic parameters were estimated in the presence of 40 mmol kg^{-1} $P(OMe)_3$ in the bulk. [e] The dissociation constant, K, was $(2.5 \pm 0.1) \times 10^{-3}$ at 313.1 K with $\Delta H° = 19.5$ kJ mol^{-1} and $\Delta S° = -112$ J mol^{-1} K^{-1}.

$$trans\text{-}[Co(dtc)_2(\text{P-ligand})_2]^+ \overset{K}{\rightleftharpoons} trans\text{-}[Co(dtc)_2(\text{P-ligand})]^+(A) + \text{P-ligand} \qquad (1')$$

As the ligand-field of $P(OMe)_3$ is larger than those of $P(OMe)_2Ph$ or $P(OMe)Ph_2$, the k_2 process that leads to isomerization is not important for this reaction either.[12,13] Furthermore, the saturation behavior up to $[P(OMe)_3]_{free} = 40$ mmol kg^{-1} indicates that the dissociation of coordinated $P(OMe)_3$ is significant: the NMR result shown in Fig. 7 also indicates the significant degree of dissociation of coordinated $P(OMe)_3$. However, it should be noted that the reaction was first-order even under the conditions where dissociation of $P(OMe)_3$ is not completely suppressed ($[P(OMe)_3]_{free} < 40$ mmol kg^{-1}). Such an observation leads to the conclusion that the decomposition of 5-coordinate intermediate (A) takes place through further dissociation of coordinated $P(OMe)_3$, which is completely suppressed by the addition of excess free $P(OMe)_3$. Therefore, we suggest here that a dead-end mechanism involving (i) the formation of the non-reactive 5-coordinate $[Co(dtc)_2\{P(OMe)_3\}]^+$ and (ii) the intramolecular twist process by reaction (3): the observed pseudo-first-order rate constant is described by the following equation.

$$k_{obs} = \frac{k_3[P(OMe)_3]_{free}}{K + [P(OMe)_3]_{free}} \qquad (6)$$

The dissociation constant, K, was estimated as 2.5×10^{-3} mol kg^{-1} at 313 K from the plots in Fig. 9. This value of K estimates that 76% dissociation of coordinated $P(OMe)_3$ is expected in a 1 mmol kg^{-1} solution of *trans*-$[Co(dtc)_2\{P(OMe)_3\}_2]^+$, and that *ca.* 6% dissociation takes place even under the condition of $[P(OMe)_3]_{free} = 40$ mmol kg^{-1}.

The rate constants and activation parameters for the isomerization reactions of *trans*-$[Co(dtc)_2\{P(OMe)_{3-n}Ph_n\}_2]^+$ are summarized in Table 6. The activation parameters of these reactions are consistent with those reported for the ordinary intramolecular process (Ray–Dutt type twist mechanism[30,31]), including the previously reported intramolecular isomerization reaction of *trans*-$[Co(dtc)_2(PHPh_2)_2]^+$:[9a] a large activation enthalpy with near-zero activation entropy.[32,33] The AOM calculation for the twist mechanism also indicates that the reaction proceeds *via* a spin state change: the process through the spin-quintet state of the trigonal prismatic transition state is energetically more favorable compared with the process in which the spin-singlet state is maintained during the activation process.[9a,11,13]

The difference between eqns. (5) and (6) depends solely on the following assumptions: when $k_1 \ll k_{-1}[P(OMe)_3]_{free}$, eqn. (5) is valid as the steady state approximation is effective for the 5-coordinate species; while the rapid equilibrium in eqn. (1′) ensures the relation, $k_3 \ll k_1 + k_{-1}[P(OMe)_3]_{free}$, where K is defined by k_1/k_{-1}.[11,34] As K is 2.5×10^{-3} kg mol^{-1} at 313 K, the inequality is expressed by $k_3 \ll k_{-1}(2.5 \times 10^{-3} + [P(OMe)_3]_{free})$. This inequality is fulfilled when k_3 is small, which is the case observed in this study: $k_3 = 4.22 \times 10^{-4}$ s^{-1} at 313 K.[35] Moreover, we can safely infer that the dissociation rate constant, k_1, for $P(OMe)_3$ is the largest of the three reactions examined in this study (K is the largest for *trans*-$[Co(dtc)_2\{P(OMe)_3\}_2]^+$ while k_{-1} is assumed to be the same for all reactions): the kinetic *trans* effect is in the order of $P(OMe)_3 \gg P(OMe)Ph_2$, $P(OMe)_2Ph$, and $PHPh_2$.

The dissociation rate constants for the $P(OMe)Ph_2$ and $P(OMe)_2Ph$ complexes, k_1, were roughly estimated as $\approx 10^{-4}$ and $\approx 10^{-6}$ s^{-1} at 298 K, respectively, by the double-exponential analyses of the kinetic trace when no free P-ligand was added to each sample solution. The previously obtained rate constant for the dissociation of coordinated $PHPh_2$ from *trans*-$[Co(dtc)_2(PHPh_2)_2]^+$, $\approx 10^{-5}$ s^{-1} at 298 K,[9a] is exactly in between those for

the $P(OMe)Ph_2$ and $P(OMe)_2Ph$ complexes. This order in the dissociation rate constant is consistent with the expected order of π-acidity for these P-ligands: $P(OMe)_2Ph > PHPh_2 > P(OMe)Ph_2$, by considering the small pK_a values of the conjugate acids and the decreasing value of the χ parameters for these P-ligands. Such a result indicates that the π-acidity of the P-ligand plays a significant role in the kinetic *trans* effect observed for *trans*-$[Co(dtc)_2(P\text{-ligand})_2]^+$ in solution.

The static *trans* influence was examined on the basis of the Co–P bond length and the ligand-field parameter, Δ, as mentioned in the previous section. It was shown in Figs. 2 and 5b that the *trans* influence in the series of *trans*-$[Co(dtc)_2(P\text{-ligand})_2]^+$ is essentially explained by Tolman's cone angle: $P(OMe)Ph_2 > P(OMe)_2Ph > P(OMe)_3$. The kinetic results, however, indicate that the *trans* effect is the largest for $P(OMe)_3$. Therefore, it seems that the Co–P bond length is not directly related to the kinetic *trans* effect: it seems that the kinetic *trans* effect for this series of P-ligand complexes is governed by the stability of the 5-coordinate species (A). On the basis of the AOM calculations, it has already been reported that the energy difference between the d^6 cobalt(III) ions in the pseudo-octahedral coordination geometry and in the pseudo-square pyramidal coordination geometry is essentially described by the π-interaction energy, $\Delta E \approx -4e_\pi$:[36] the larger the π-acidity of the P-ligand, the less stabilization of the 5-coordinate species is indicated. Such a tendency is opposite to the order of the observed kinetic *trans* effect. Therefore, a comprehensive understanding of the kinetic *trans* effect observed for the series *trans*-$[Co(dtc)_2(P\text{-ligand})_2]^+$ requires consideration of not only the effect of the P-ligands but also the effect of the spectator ligands.

The chemical shift of the $P–OCH_3$ proton (Table 1) does not seem to directly reflect the electron density on the P-ligand in the 6-coordinate species. On the other hand, the ^1H NMR signal of $N–CH_3$ moiety as a function of the P-ligands were observed at 2.39, 2.72, 2.99, and 3.31 ppm for PPh_3, $P(OMe)Ph_2$, $P(OMe)_2Ph$, and $P(OMe)_3$ complexes, respectively (Table 1), which may reflect the gradual decrease of electron density on dtc^- in this order. Therefore, it seems that the spectator ligand, dtc^-, supplies more electron density to the cobalt(III) center as the π-acidity of the P-ligand increases. Such a capability of the dtc^- ligand to act as an electron sponge certainly stabilizes cobalt(III) complexes with π-acids by altering the electron density on Co. This seems to be the main reason why the Co–P bond lengths as well as the ligand-field strengths, Δ, do not linearly depend on the electronic parameter, χ, of the P-ligand. However, such an effect of dtc^- as an electron sponge may not be strong enough to compensate for the decrease in the electron density on cobalt(III) in the *trans*-$[Co(dtc)_2\{P(OMe)_3\}_2]^+$ complex, since the π-acidity of $P(OMe)_3$ is much larger than those for $P(OMe)_2Ph$ and $P(OMe)Ph_2$: χ = 24.10, 19.45, and 16.30 for $P(OMe)_3$, $P(OMe)_2Ph$, and $P(OMe)Ph_2$, respectively. As a result, the 5-coordinate species, $[Co(dtc)_2\{P(OMe)_3\}]^+$, is largely stabilized compared with the other 5-coordinate species in which the P-ligand is $P(OMe)_2Ph$ or $P(OMe)Ph_2$. In such a case, the $P–OCH_3$ ^1H NMR signal of the 5-coordinate species should be observed at a higher-field than that for the 6-coodinate species since the loss of one of the $P(OMe)_3$ ligands stabilizes another Co–P bond through the enhancement of the π-interaction. In fact, the ^1H NMR signal corresponding to the coordinated $P(OMe)_3$ appeared at 3.68 ppm in Fig. 7. The lower-field shift of the $N–CH_3$ protons on dtc^- in Fig. 7 indicates stabilization of the cobalt(III) center in the 5-coordinate $[Co(dtc)_2\{P(OMe)_3\}]^+$ by the electron sponge effect of this spectator ligand.

The AOM calculation also implies that the activation enthalpy for the twist process increases with increasing ligand-field parameter, Δ, when the electron pairing energy is the same for all complexes.[9a,37] As the activation enthalpies for the twist processes of $P(OMe)_{3-n}Ph_n$ complexes roughly followed the order of Δ for these complexes, the electron sponge effect of the dtc^- ligand seems to equally affect the energy levels of the ground state and the trigonal prismatic transition state.

Conclusion

In this study, a series of *trans*- and *cis*-$[Co(dtc)_2\{P(OMe)_{3-n}Ph_n\}_2]^+$ complexes were synthesized and the structures of related *trans*- and *cis*-$[Co(dtc)_2(P\text{-ligand})_2]^+$ complexes were examined. It was found that the Co–P bond lengths as well as the ligand-field parameters were primarily governed by the steric bulk of the P-ligand, the cone angle. It was also shown that the complexes of P-ligands with strong σ-donicity (PMe_3) and strong π-acidity ($P(OMe)_3$) are equally stabilized. Such a tendency was clearly seen in Figs. 5a and b with the inflection point at the PPh_3 ligand, for which the cone angle is the largest of all P-ligands while both σ-donicity and π-acidity are not eminent. The very labile nature of the PPh_3 complex, which was exploited for the efficient syntheses of the other *trans*-bis-(P-ligand) complexes, may be explained by the relatively weak $Co–PPh_3$ bond caused by the very large cone angle of this ligand. Otherwise, the almost identical stability of the Co–P bonds for the series of *trans*- and *cis*-$[Co(dtc)_2(P\text{-ligand})_2]^+$ complexes is explained by the electron sponge effect of the spectator ligand, dtc^-.

The kinetic studies of the thermal *trans* to *cis* isomerization reactions of these complexes revealed that the reactions proceed through the intramolecular twist mechanism. A significant degree of dissociation of coordinated $P(OMe)_3$ was observed for *trans*-$[Co(dtc)_2\{P(OMe)_3\}_2]^+$. This strong (kinetic) *trans* effect in *trans*-$[Co(dtc)_2\{P(OMe)_3\}_2]^+$ was attributed to the stabilization of the 5-coordinate $[Co(dtc)_2\{P(OMe)_3\}]^+$ caused by the combination of strong π-acidity inherent in $P(OMe)_3$ and the electron sponge effect of the spectator ligand, dtc^-.

References and notes

1 T. Ohishi, K. Kashiwabara and J. Fujita, *Bull. Chem. Soc. Jpn.*, 1987, **60**, 583.
2 M. Kita, A. Okuyama, K. Kashiwabara and J. Fujita, *Bull. Chem. Soc. Jpn.*, 1990, **63**, 1994.
3 M. Adachi, M. Kita, K. Kashiwabara, J. Fujita, N. Iitaka, S. Kurachi and S. Ohba, *Bull. Chem. Soc. Jpn.*, 1992, **65**, 2037.
4 M. Kita, M. Okuno, K. Kashiwabara and J. Fujita, *Bull. Chem. Soc. Jpn.*, 1992, **65**, 3042.
5 H. Matsui, M. Kita, K. Kashiwabara and J. Fujita, *Bull. Chem. Soc. Jpn.*, 1993, **66**, 1140.
6 K. Kashiwabara, M. Watanabe, M. Kita and T. Suzuki, *Bull. Chem. Soc. Jpn.*, 1996, **69**, 1947.
7 K. Kashiwabara, N. Taguchi, H. D. Takagi, K. Nakajima and T. Suzuki, *Polyhedron*, 1998, **17**, 1817.
8 T. Suzuki, S. Kashiwamura and K. Kashiwabara, *Bull. Chem. Soc. Jpn.*, 2001, **74**, 2349.
9 (*a*) S. Iwatsuki, T. Suzuki, A. Hasegawa, S. Funahashi, K. Kashiwabara and H. D. Takagi, *J. Chem. Soc., Dalton Trans.*, 2002, 3593; (*b*) T. Suzuki, S. Iwatsuki, H. D. Takagi and K. Kashiwabara, *Chem. Lett.*, 2001, 1068.
10 (*a*) H.-Y. Liu, K. Eriks, A. Prock and W. P. Giering, *Organometallics*, 1990, **9**, 1758; (*b*) Md. M. Rahman, H.-Y. Liu, K. Eriks, A. Prock and W. P. Giering, *Organometallics*, 1989, **8**, 1.
11 R. B. Jordan, *Reaction Mechanisms of Inorganic and Organometallic Systems*, Oxford University Press, Oxford, 2nd edn., 1998.
12 L. G. Vanquickenborne and K. Pierloot, *Inorg. Chem.*, 1981, **20**, 3673.
13 L. G. Vanquickenborne and K. Pierloot, *Inorg. Chem.*, 1984, **23**, 1471.
14 (*a*) N. N. Greenwood and A. Earnshaw, *Chemistry of the Elements*, Butterworth-Heinemann, Oxford, 2nd edn., 1997; (*b*) J. E. Huheey, *Inorganic Chemistry*, Harper & Row, New York, 2nd edn., 1978.
15 C. A. Tolman, *Chem. Rev.*, 1977, **77**, 313.
16 P. Coppens, L. Leiserowitz and D. Rabinovich, *Acta Crystallogr., Sect. A*, 1965, **18**, 1035.
17 A. C. T. North, D. C. Phillips and F. S. Mathews, *Acta Crystallogr., Sect. A*, 1968, **24**, 351.

18 Rigaku Co. Ltd., CrystalClear, Control program for Rigaku Mercury CCD diffractometer, Akishima, Tokyo, Japan, 2001.
19 T. Higashi, abscor, empirical absorption correction based on Fourier series approximation, Rigaku Corp., Tokyo, Japan, 1995.
20 G. M. Sheldrick, *Acta Crystallogr., Sect. A*, 1990, **46**, 467.
21 G. M. Sheldrick, SHELXS97 and SHELXL97, University of Göttingen, Germany, 1997.
22 Molecular Structure Corporation and Rigaku Co. Ltd., TeXsan, Single crystal structure analysis software, ver. 1.9, The Woodlands, TX, USA and Akishima, Tokyo, Japan, 1998.
23 T. Suzuki, S. Kaizaki and K. Kashiwabara, *Inorg. Chim. Acta*, 2000, **298**, 131.
24 (*a*) N. Bresciani-Pahor, M. Forcolin, L. G. Marzilli, L. Randaccio, M. F. Summers and P. J. Toscano, *Coord. Chem. Rev.*, 1985, **63**, 1; (*b*) N. Bresciani-Pahor, L. Randaccio and P. J. Toscano, *J. Chem. Soc., Dalton Trans.*, 1982, 1559; (*c*) N. Bresciani-Pahor, L. Randaccio, P. J. Toscano, A. C. Sandercock and L. G. Marzilli, *J. Chem. Soc., Dalton Trans.*, 1982, 129.
25 T. Suzuki, K. Kashiwabara, M. Kita, J. Fujita and S. Kaizaki, *Inorg. Chim. Acta*, 1998, **281**, 77.
26 T. Suzuki, T. Imamura, S. Kaizaki and K. Kashiwabara, *Polyhedron*, 2002, **21**, 835.
27 (*a*) J. M. Smith, N. J. Coville, L. M. Cook and J. C. A. Boeyens, *Organometallics*, 2000, **19**, 5273; (*b*) T. E. Müller and D. M. P. Mingos, *Transition Met. Chem.*, 1995, **20**, 533; (*c*) J. T. DeSanto, J. A. Mosbo, B. N. Storhoff, P. L. Bock and R. E. Bloss, *Inorg. Chem.*, 1980, **19**, 3086.
28 O. Dahl and R. S. Edmundson, in *The Chemistry of Organophosphorus Compounds*, ed. F. R. Hartley, John Wiley & Sons, Chichester, 1996, vol. 4, ch. 1 and 2.
29 C. J. Pouchert and J. R. Campbell, *The Aldrich Library of NMR Spectra*, Aldrich Chemical Co. Inc., Milwaukee, 1974, vol. 10.
30 P. C. Ray and N. K. Dutt, *J. Indian Chem. Soc.*, 1941, **18**, 289.
31 P. C. Ray and N. K. Dutt, *J. Indian Chem. Soc.*, 1943, **20**, 81.
32 F. F.-L. Ho and C. N. Reilley, *Anal. Chem.*, 1969, **41**, 1835.
33 R. G. Wilkins and M. J. G. Williams, *J. Chem. Soc.*, 1957, 1763.
34 G. I. Gellene, *J. Chem. Educ.*, 1995, **72**, 196.
35 In this case, k_1 is not necessarily very large. However, we observed ^{1}H NMR signals corresponding to N–CH_3 and P–OCH_3 of the 5-coordinate species at *ca.* 3.28 and 3.68 ppm, 15 minutes after sampling the *trans*-$[Co(dtc)_2\{P(OMe)_3\}_2]^+$ solution without free $P(OMe)_3$. Therefore, k_1 is roughly estimated as 8×10^{-4} s^{-1}. Accordingly, k_{-1} is estimated as *ca.* 3 kg mol^{-1} s^{-1}, that fulfills the inequality, $k_3 \ll k_1 + k_{-1}[P(OMe)_3]_{free}$ as $[P(OMe)_3]_{free} > 5 \times 10^{-3}$ mol kg^{-1}.
36 E. Larsen and G. N. La Mar, *J. Chem. Educ.*, 1974, **51**, 633.
37 The spin-pairing energy for a d^6 configuration is somewhat reduced to a value less than 20000 cm^{-1} depending on the decrease in the inter-electronic repulsion. See: (*a*) F. A. Cotton, G. Wilkinson and P. L. Gauss, *Basic Inorganic Chemistry*, Wiley, New York, 3rd edn., 1995; (*b*) A. B. P. Lever, *Inorganic Electronic Spectroscopy*, Elsevier, Amsterdam, 2nd edn., 1984.